

Detection of Impaired OFDM Waveforms Using Deep Learning Receiver

Jaakko Pihlajasalo¹, Dani Korpi², Taneli Riihonen¹, Jukka Talvitie¹, Mikko A. Uusitalo², and Mikko Valkama¹
¹Electrical Engineering, Tampere University, Finland ²Nokia Bell Labs, Espoo, Finland

Abstract—With wireless networks evolving towards mmWave and sub-THz frequency bands, hardware impairments such as IQ imbalance, phase noise (PN) and power amplifier (PA) nonlinear distortion are increasingly critical implementation challenges. In this paper, we describe deep learning based physical-layer receiver solution, with neural network layers in both time- and frequency-domain, to efficiently demodulate OFDM signals under coexisting IQ, PN and PA impairments. 5G NR standard-compliant numerical results are provided at 28 GHz band to assess the receiver performance, demonstrating excellent robustness against varying impairment levels when properly trained.

Index Terms—5G NR, 6G, deep learning, hardware impairments, IQ imbalance, machine learning, mmWave, nonlinear distortion, power amplifier, phase noise, sub-THz

I. INTRODUCTION

One timely paradigm in 5G evolution and 6G research is harnessing new spectrum from the 50–300 GHz bands [1], [2]. While such mmWave or sub-THz bands can offer large channel bandwidths and thereon improved capacity and latency characteristics, the use of such bands for mobile radio access imposes also substantial technical challenges, including the quality, cost- and energy-efficiency of the electronics [2], [3], the extreme path loss and propagation characteristics [4] and the overall system complexity and deployment costs to provide indoor and outdoor network coverage with mobility support. To this end, the combination of extremely wide channel bandwidths and high center-frequencies pushes the performance boundaries of the involved electronics, particularly data converters, transceivers, oscillators and power amplifiers to their limits, with challenging tradeoffs in the corresponding integrated circuit size, design and implementation costs, as well as the energy consumption [2], [5].

In this work, we investigate and develop solutions for utilizing modern machine learning (ML) techniques to reliably demodulate received signals under severe levels of radio frequency (RF) impairments. Building on top of our prior work in [6], we consider the challenging case of co-existing power amplifier (PA) nonlinear distortion, inphase/quadrature (IQ) imbalance and oscillator phase noise (PN), and devise a hybrid time-/frequency-domain neural network (NN) structure and associated learning procedures facilitating reliable detection of the information bits from the distorted time-domain IQ signal. Extensive set of numerical results conforming to the current 5G New Radio (NR) mmWave specifications are provided, demonstrating the successful operation of the developed receiver system under varying levels of the involved RF imperfections. Such receiver technology can provide native

ML support for the 6G physical layer, while allowing to improve the network coverage, energy-efficiency and cost-efficiency.

Notation: Matrices are represented with boldface uppercase letters and they can consist of either real- or complex-valued elements, i.e., $\mathbf{X} \in \mathbb{F}^{N \times M}$, where \mathbb{F} stands for either \mathbb{R} or \mathbb{C} .

II. STATE-OF-THE-ART

ML-aided radio reception has already been considered in several works, some of which have investigated implementing certain parts of the receiver chain with learned layers [7]–[9], while some works have learned the complete receiver from data [10]–[12]. Such fully learned receivers have demonstrated high performance especially under sparse pilot configurations or when the cyclic prefix is omitted. In addition, the solution in [12] is shown to be capable of dealing rather well with transmitter clipping noise, a type of hard nonlinearity.

The prospect of hardware impairments has also been analyzed in the context of ML-based receiver solutions. In addition to our earlier work on mitigating transmitter PA-induced distortion [6], [13], there are some existing works focusing on PN and IQ imbalance [14]–[17]. In particular, [14] proposes an ML-based channel estimator under PN and IQ imbalance, demonstrating higher accuracy than conventional methods. The work in [15], on the other hand, describes a fully learned receiver that can operate under IQ imbalance and carrier frequency offset. The ML-based receiver architecture proposed therein utilizes a parallel structure, shown to outperform the conventional baseline receiver. The issue of PN in sub-THz frequency bands is addressed in [16] by using a deep NN receiver solution. The proposed NN receiver takes in the received signal and a channel estimate, and provides a hard symbol decision as its output, achieving lower bit error rates than the baseline solution. Finally, the work in [17] investigates another type of PN resistant ML receiver, consisting of separate NN elements trained to carry out channel estimation and data detection. It is shown that introducing an additional NN for mitigating the effects of PN results in higher detection accuracy.

As opposed to any of these earlier works, in this paper we provide methods and results for a scenario where all dominant impairment sources are jointly present. That is, we devise, train and evaluate the performance of the fully learned receiver solutions under the joint effect of PN, IQ imbalance, and PA-induced nonlinearities. Moreover, unlike in most prior works, the training and validation data is generated under varying

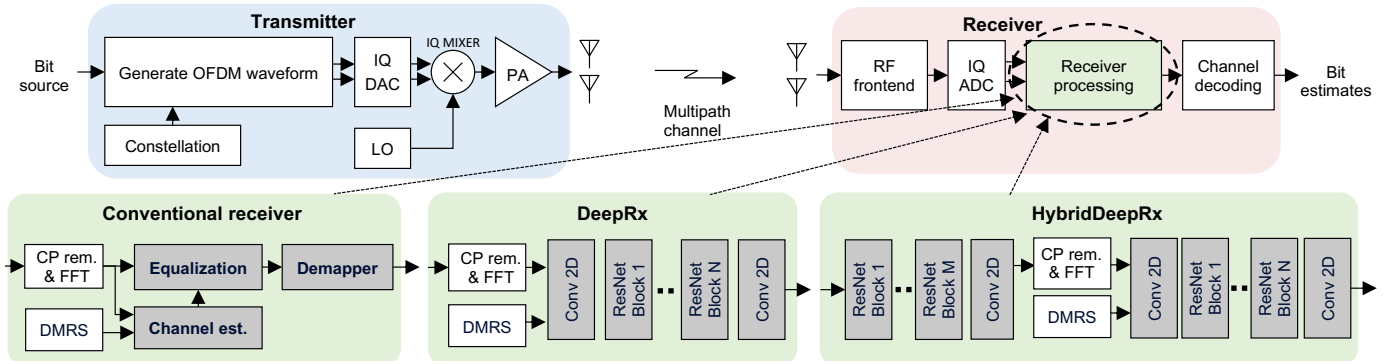


Fig. 1. High-level illustration of the considered system, where the transmitter is producing IQ imbalance and PN in the upconversion phase, and nonlinear distortion at the power amplifier. This work considers three different receiver systems, each depicted in the lower part of the figure.

impairment levels, instead of a static scenario. Therefore, the reported performance results correspond to a more practical scenario, with large anticipated technological relevance. It is shown that HybridDeepRx [6] like receivers with properly trained NN layers in both time- and frequency-domain can handle the challenging combination of co-existing RF impairments and mobile multipath channel, clearly outperforming the ordinary DeepRx [10].

III. SYSTEM MODEL

The system model is depicted in Fig. 1, illustrating both the transmit and receiver side processing. We consider a 5G-type scenario, although the proposed deep learning receiver architecture is also a promising candidate for beyond 5G and 6G systems [13]. Therefore, the transmitter produces an orthogonal frequency-division multiplexing (OFDM) waveform and follows a typical direct-conversion architecture in the RF domain. Denoting the ideal time-domain transmit waveform by $x(n)$, the baseband-equivalent transmit signal after the IQ upconversion can be written as

$$x_{IQ}(n) = (K_1x(n) + K_2x^*(n))e^{j\theta(t)}, \quad (1)$$

where $\theta(t)$ is the PN term, and the IQ imbalance coefficients are defined as $K_1 = (1 + g\exp(-i\phi))/2$ and $K_2 = (1 - g\exp(i\phi))/2$, with g and ϕ denoting the amplitude and phase imbalances, respectively ($g = 1$ and $\phi = 0$ correspond to a case with no IQ imbalance). Note that in this work we assume the IQ imbalance to be frequency-independent, while the PN is modeled based on a free-running oscillator (FRO) model.

After this, the upconverted RF signal is fed to the nonlinear power amplifier, and the final transmit signal is given by

$$x_{RF}(n) = \sum_{\substack{p=1 \\ p \text{ odd}}}^P f_p |x_{IQ}(n)|^{p-1} x_{IQ}(n) \quad (2)$$

where P is the nonlinearity order of the model and f_p denotes the p th-order coefficient of the polynomial model.

This transmit signal then experiences a mobile multipath channel while propagating to the receiver, after which the received signal can be written as follows:

$$y(n) = \sum_{m=0}^{M-1} h_{m,n} x_{RF}(n-m) + w(n), \quad (3)$$

where $h_{m,n}$ denotes the time-varying M -path channel impulse response, and $w(n)$ is the noise-plus-interference signal.

Considering the signal during a single transmission time interval (TTI), the received time-domain signal can be denoted by a matrix $\mathbf{Y}_t \in \mathbb{C}^{(N_{CP}+N) \times N_{\text{syemb}}}$, where N_{CP} is the maximum cyclic prefix (CP) length within the TTI, N is the fast Fourier transform (FFT) size and N_{syemb} is the number of OFDM symbols. That is, the elements of \mathbf{Y}_t consist simply of the received signal samples, ordered based on their corresponding OFDM symbols. In case the symbols have different CP lengths, as is often the case in 5G, zero-padding is used to align the total symbol lengths to $N_{CP} + N$.

After removing the CP, the received signal can be converted to frequency domain using a fast Fourier transform (FFT). With this, the received frequency domain signal can be written as

$$\mathbf{Y} = \mathbf{H} \circ \mathbf{X} + \mathbf{N}, \quad (4)$$

where $\mathbf{Y} \in \mathbb{C}^{N_D \times N_{\text{syemb}}}$ and $\mathbf{X} \in \mathbb{C}^{N_D \times N_{\text{syemb}}}$ are the received and transmitted OFDM symbols in frequency domain, respectively, $\mathbf{H} \in \mathbb{C}^{N_D \times N_{\text{syemb}}}$ is the frequency-domain single-tap channel matrix, $\mathbf{N} \in \mathbb{C}^{N_D \times N_{\text{syemb}}}$ is the noise-plus-interference signal, and N_D denotes the number of allocated subcarriers. Note especially that the noise terms in \mathbf{N} contain also all the distortion components stemming from IQ imbalance, PN, PA nonlinearities, and inter-carrier interference (ICI) meaning that it is a function of the original TX signal. A conventional linear receiver interprets such components as noise, while the proposed ML-based receiver will learn to model and mitigate these distortions.

Such a conventional receiver is utilized in this work as a baseline to provide the proper comparison and context for the performance of the ML-based DeepRx. In the baseline receiver, the demodulation reference signals (DMRSs) are

extracted from the pilot-carrying OFDM symbols in \mathbf{Y} for channel estimation, as illustrated in Fig. 1, after which the signal is equalized and the soft bits, or log-likelihood ratios (LLRs), are extracted. For a more detailed description of the baseline receiver, see, e.g., [10].

IV. CONSIDERED ML-BASED RECEIVERS AND DATA GENERATION

The goal of the proposed ML-based receivers is to detect the bits from the impaired RX signals collected during a transmission time interval (TTI). In this work, we consider two ML-based receivers: DeepRx [10] and HybridDeepRx [6]. DeepRx is a deep learning receiver with trainable convolutional layers in the frequency-domain, while HybridDeepRx has trainable convolutional layers both in the time- and frequency-domain. The time-domain layers are well-suited for mitigating the non-linear impairments that are inherently time-domain phenomena such as IQ imbalance and PA distortion. Similarly, the layers in the frequency-domain will mitigate frequency-domain impairments while simultaneously performing channel estimation and the actual signal detection. The general architectures of both receiver solutions are presented in Fig. 1.

Considering first the inputs of the two ML-based receivers, the input of the frequency-domain DeepRx consists of the post-FFT received signal $\mathbf{Y} \in \mathbb{C}^{N_D \times N_{\text{symp}}}$ and the raw least squares (LS) DMRS channel estimates $\hat{\mathbf{H}} \in \mathbb{C}^{N_D \times N_{\text{symp}}}$, where the latter has been filled with zeros for the non-DMRS REs. The real and imaginary parts of the inputs are concatenated along the third input dimension to construct the full input array $\mathbf{Z} \in \mathbb{R}^{N_D \times N_{\text{symp}} \times 4}$.

As opposed to this, HybridDeepRx takes as input the time-domain received signal with the CPs, denoted by $\mathbf{Y}_t \in \mathbb{C}^{(N_{CP}+N) \times N_{\text{symp}}}$, as well as the frequency-domain DMRS channel estimates $\hat{\mathbf{H}} \in \mathbb{C}^{N_D \times N_{\text{symp}}}$. The time-domain RX signal is fed directly to the time-domain layers as a real-valued array $\mathbf{Z}_1 \in \mathbb{R}^{(N+N_{CP}) \times N_{\text{symp}} \times 2}$, while the channel estimates are fed to the frequency-domain part of the ML receiver, also as a real-valued array $\mathbf{Z}_2 \in \mathbb{R}^{(N_D) \times N_{\text{symp}} \times 2}$.

The outputs of both trained receivers are real-valued arrays $\mathbf{L} \in \mathbb{R}^{N_D \times N_{\text{symp}} \times B}$ consisting of the estimated LLRs, where B is the number of bits per RE. The bit estimates are obtained by feeding the LLRs through the sigmoid-function. Note that the convolutional ML receivers estimate LLRs also for the DMRS-carrying REs, but these are naturally discarded.

In this work, we consider three scenarios with varying impairments affecting the signals: (1) a PN only scenario, (2) an IQ imbalance only scenario, and (3) a scenario including all impairment sources, i.e., PN, IQ imbalance, and the PA-induced nonlinearities. The impairments are modeled according to the signal model presented in section III with parameter ranges specified in Table I for the training datasets. For validation, we utilize separate datasets with similar parameter ranges, as well as datasets with fixed impairment parameters. The PA models used in training and validation are varied by dithering a measured polynomial PA model to ensure that

TABLE I
IMPAIRMENT PARAMETER RANGES FOR TRAINING. THE RANGES CORRESPOND TO THE BOUNDS OF A UNIFORM DISTRIBUTION

| | Phase noise 3dB bandwidth | Amplitude imbalance | Phase imbalance | PA output backoff |
|------------|------------------------------|------------------------|--------------------|----------------------|
| Scenario 1 | 1 Hz to 20 Hz | N/A | N/A | N/A |
| Scenario 2 | N/A | -15% to 15% | -15° to 15° | N/A |
| Scenario 3 | 1 Hz to 20 Hz | -15% to 15% | -15° to 15° | 3 dB |

TABLE II
MMWAVE SIMULATION PARAMETERS FOR TRAINING AND VALIDATION

| Parameter | Value | Randomization |
|----------------------------------|--------------------|-----------------------|
| Center frequency | 28 GHz | None |
| Channel model | TDL-A to TDL-E | Uniform distribution |
| PA model | Measured | Dithered coefficients |
| SNR | 0 dB – 30 dB | Uniform distribution |
| Doppler shift | 0 Hz – 1500 Hz | Uniform distribution |
| Delay spread | Up to 100 ns | Uniform distribution |
| Channel bandwidth | 50 MHz | None |
| Number of subcarriers (N_D) | 792 subcarriers | None |
| FFT size (N) | 1024 | None |
| Subcarrier spacing | 60 kHz | None |
| Maximum CP length (N_{CP}) | 104 | None |
| TTI length (N_{symp}) | 14 OFDM symbols | None |
| DMRS configuration | 2 OFDM symb. / TTI | None |
| Modulation scheme | 64-QAM | None |

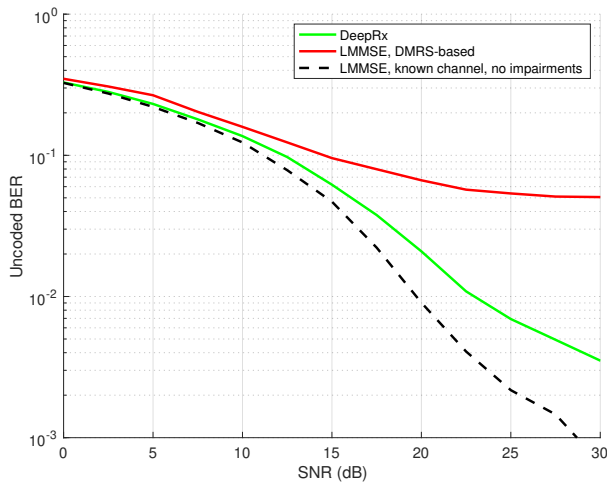
the neural network generalizes properly. For further details on utilized PA models, we refer to [6].

To generate data, we employ Matlab's 5G Toolbox [18] to simulate a 5G physical uplink shared channel (PUSCH) link. Parameters for the simulation are specified in Table II. The training dataset for each scenario utilizes a randomly chosen tapped delay line (TDL) channel model among TDL-B, TDL-C and TDL-D [19] models while the validation datasets utilize TDL-A and TDL-E models. For training, the SNR is chosen randomly, while for the validation the SNRs are in uniform grid with 2.5 dB steps in the specified range. The training datasets consist of 105 000 TTIs whereas the validation datasets consists of 32 000 TTIs.

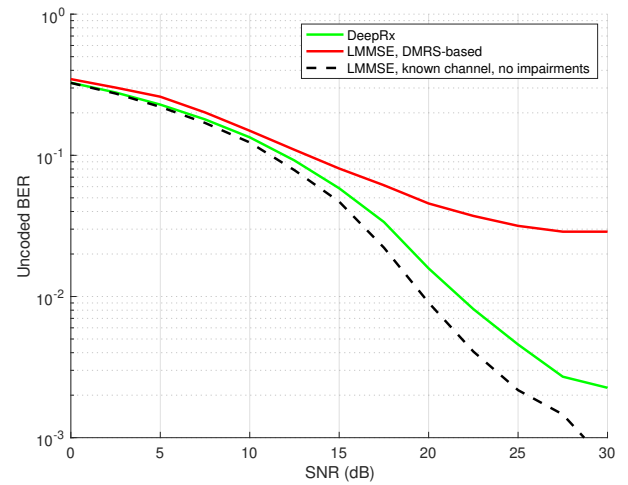
The training of ML receivers is performed based on the binary cross entropy (CE) loss between the estimated bits and the transmitted bits, similar to [10]. The CE loss is defined as

$$\text{CE}(\boldsymbol{\theta}) \triangleq -\frac{1}{\#\mathcal{D}B} \sum_{(i,j) \in \mathcal{D}} \sum_{l=0}^{B-1} \left(b_{ijl} \log(\hat{b}_{ijl}) + (1 - b_{ijl}) \log(1 - \hat{b}_{ijl}) \right) \quad (5)$$

where $\boldsymbol{\theta}$ represents the set of trainable of parameters, \mathcal{D} denotes the time and frequency indices of data-carrying resource elements (RE), $\#\mathcal{D}$ is the total number of data-carrying REs, B is the number of bits per RE, and \hat{b}_{ijl} is the receiver's estimate for the probability that the bit b_{ijl} is one. We use Adam optimizer as the stochastic gradient descent (SGD) algorithm for learning the model parameters.

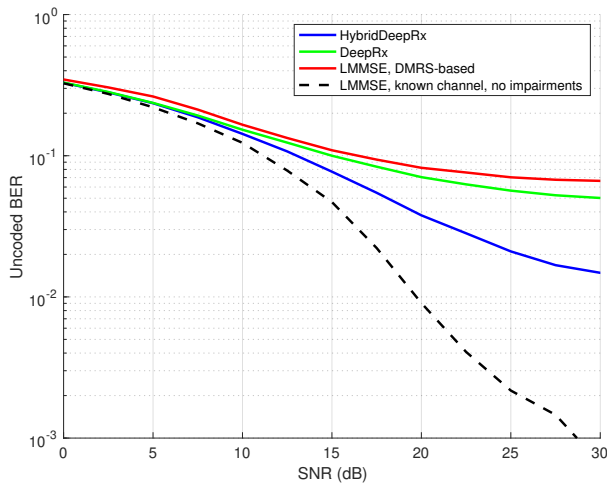


(a) 3dB bandwidth of 20 Hz

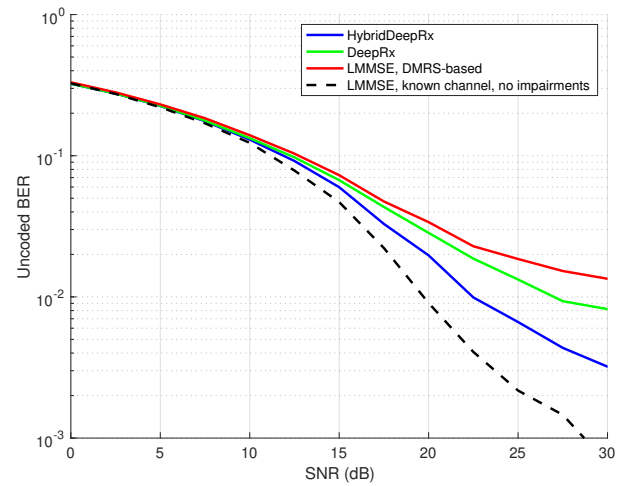


(b) 3dB bandwidth $\sim U(1, 20)$ Hz

Fig. 2. The BER performance of the considered receivers with phase noise affecting the signals for both validation scenarios.



(a) $g = 1.15, \phi = 15^\circ$



(b) $g \sim U(0.85, 1.15), \phi \sim U(-15^\circ, 15^\circ)$

Fig. 3. The BER performance of the considered receivers under IQ imbalance for both validation scenarios.

V. PERFORMANCE EVALUATION

The performance of the ML-based receivers is first evaluated under Scenarios 1 and 2 after which we investigate the Scenario 3 with all impairments simultaneously present. Uncoded bit error rate (BER) is considered the main performance criteria, the results of the deep learning receivers being compared with a baseline receiver utilizing linear minimum mean square error (LMMSE) equalization and least squares (LS) channel estimation. In addition, we include as a reference the BER achieved by an LMMSE based receiver with known channel and without any impairments, representing essentially the performance bound.

Fig. 2 shows the BER performance of DeepRx under Scenario 1 for the PN impaired signals under FRO 3dB bandwidth of a) 20 Hz and b) 1-20 Hz with uniformly distributed values. It was observed that the performance of DeepRx and HybridDeepRx was essentially identical in this scenario, hence HybridDeepRx is not presented in the figures. In both cases,

we can see that DeepRx can mitigate the PN considerably well. This is because it has the structural capability to learn and suppress ICI within neighboring subcarriers induced by PN. It outperforms the LMMSE-based receiver by a clear margin, and is not far behind the ideal baseline even with the most severe PN case in Fig. 2a.

In Fig. 3 we see the BER performance of the considered receivers under Scenario 2 with the IQ imbalance impaired signals, when considering a) fixed and b) randomized imbalance parameters. Fig. 3a shows the performance when amplitude and phase imbalances are fixed at 15% and 15° respectively, which corresponds to an image rejection ratio (IRR) of 16.5 dB. Correspondingly, Fig. 3b shows the BERs when the imbalance parameters are uniformly distributed on the specified interval, with mean IRR of 22.9 dB. To provide some context for the IRR values, over 99% of the possible IRR values are between 16.5 to 40 dB with the considered parameter ranges. In both cases, HybridDeepRx has better

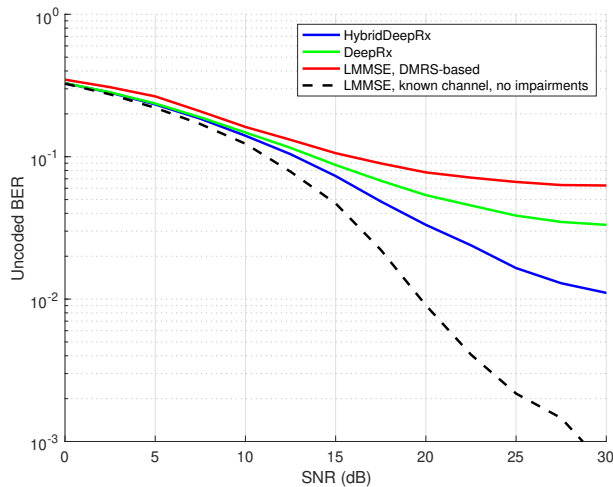


Fig. 4. The BER performance of the considered receivers with coexisting PN, IQ imbalance and PA nonlinearity. The impairment parameters are randomized as in the training dataset.

performance than other considered receivers, even in the most severe imbalance considered. This is due to frequency-domain IQ imbalance resulting in mirrored spectrum being overlapped on top of the original spectrum, making it ill-suited for convolutional processing. Hence, HybridDeepRx learns to deal with IQ imbalance more efficiently by utilizing its time-domain layers. Note that even though HybridDeepRx has more parameters than DeepRx due to the time-domain layers, adding layers with same number of parameters to the frequency side does not significantly affect the performance of the DeepRx.

Finally, we consider Scenario 3 with all the impairments present simultaneously, meaning that the signal is distorted by PN, IQ imbalance, and PA nonlinearities. Fig. 4 shows that the BER performance of the considered ML-based receivers is better than that of the conventional LMMSE-based one. Again, HybridDeepRx clearly outperforms DeepRx in this challenging scenario, as the time-domain NN layers are able to mitigate both IQ imbalance and PA distortion much more efficiently. Altogether, Fig. 4 demonstrates the resilience of the ML-based receivers, particularly that of HybridDeepRx, against various types of hardware impairments.

VI. CONCLUSIONS

In this paper, we demonstrated how different ML-based receiver architectures can be trained to deal with various hardware impairments. Our study covered two ML-based receivers, one of which is operating only in the frequency domain (DeepRx), and another one that has processing layers both in time and frequency domains (HybridDeepRx). We provided extensive numerical results in 28 GHz mmWave network context, which indicate that a frequency-domain neural network is well-suited for mitigating the effects of PN, whereas a hybrid time/frequency-domain network is required for dealing with IQ imbalance and nonlinear distortion. The results also indicated that both ML-based receivers outperform conventional baseline receivers in the appropriate impairment

scenarios. This demonstrates the resilience of the ML-based receivers against various types of hardware impairments.

ACKNOWLEDGMENT

This work was supported in part by Nokia Bell Labs and in part by the Academy of Finland under the grants #319994, #332361, and #338224.

REFERENCES

- [1] H. Tataria, M. Shafi, A. Molisch, M. Dohler, H. Sjoland, and F. Tufveson, "6G Wireless Systems: Vision, Requirements, Challenges, Insights, and Opportunities," *Proceedings of the IEEE*, Feb. 2021.
- [2] U. Gustavsson, P. Frenger, C. Fager, T. Eriksson, H. Zirath, F. Dielacher, C. Studer, A. Pärssinen, R. Correia, J. N. Matos, D. Belo, and N. B. Carvalho, "Implementation Challenges and Opportunities in Beyond-5G and 6G Communication," *IEEE Journal of Microwaves*, vol. 1, no. 1, pp. 86–100, 2021.
- [3] T. Levanen, O. Tervo, K. Pajukoski, M. Renfors, and M. Valkama, "Mobile communications beyond 52.6 GHz: Waveforms, numerology, and phase noise challenge," *IEEE Wireless Communications*, vol. 28, no. 1, pp. 128–135, 2021.
- [4] T. S. Rappaport, Y. Xing, G. R. MacCartney, A. F. Molisch, E. Mellios, and J. Zhang, "Overview of millimeter wave communications for fifth-generation (5g) wireless networks—with a focus on propagation models," *IEEE Transactions on Antennas and Propagation*, vol. 65, no. 12, pp. 6213–6230, 2017.
- [5] O. Tervo, T. Levanen, K. Pajukoski, J. Hulkkonen, P. Wainio, and M. Valkama, "5g new radio evolution towards sub-thz communications," in *6G SUMMIT*, 2020, pp. 1–6.
- [6] J. Pihlajasalo, D. Korpi, M. Honkala, J. M. J. Huttunen, T. Riihonen, J. Talvitie, A. Brihuega, M. A. Uusitalo, and M. Valkama, "Hybrid-DeepRx: Deep learning receiver for high-EVM signals," in *Proc. IEEE PIMRC*, 2021, pp. 622–627.
- [7] D. Neumann, T. Wiese, and W. Utschick, "Learning the MMSE channel estimator," *IEEE Transactions on Signal Processing*, vol. 66, no. 11, pp. 2905–2917, Jun. 2018.
- [8] H. He, C. Wen, S. Jin, and G. Li, "Deep learning-based channel estimation for beamspace mmWave massive MIMO systems," *IEEE Wireless Communications Letters*, vol. 7, no. 5, 2018.
- [9] Z. Chang, Y. Wang, H. Li, and Z. Wang, "Complex CNN-based equalization for communication signal," in *Proc. IEEE ICSIP*, Jul. 2019.
- [10] M. Honkala, D. Korpi, and J. M. J. Huttunen, "DeepRx: Fully convolutional deep learning receiver," *IEEE Transactions on Wireless Communications*, 2021.
- [11] D. Korpi, M. Honkala, J. M. J. Huttunen, and V. Starck, "DeepRx MIMO: Convolutional MIMO Detection with Learned Multiplicative Transformations," in *Proc. IEEE ICC*, 2021.
- [12] H. Ye, G. Y. Li, and B.-H. Juang, "Power of deep learning for channel estimation and signal detection in OFDM systems," *IEEE Communications Letters*, vol. 7, no. 1, pp. 114–117, 2018.
- [13] D. Korpi, M. Honkala, J. M. J. Huttunen, F. A. Aoudia, and J. Hoydis, "Waveform learning for reduced out-of-band emissions under a nonlinear power amplifier," 2022.
- [14] A. Mohammadian, C. Tellambura, and G. Y. Li, "Deep learning LMMSE joint channel, PN, and IQ imbalance estimator for multicarrier MIMO full-duplex systems," *IEEE Wireless Communications Letters*, vol. 11, no. 1, pp. 111–115, 2022.
- [15] S. Liu, T. Wang, and S. Wang, "Joint compensation of CFO and IQ imbalance in OFDM receiver: A deep learning based approach," in *Proc. IEEE/CIC ICC*, 2021, pp. 793–798.
- [16] H. S. Park, E.-Y. Choi, Y. S. Song, S. Noh, and K. Seo, "DNN-based phase noise compensation for sub-THz communications," in *Proc. ICTC*, 2020, pp. 866–868.
- [17] A. Mohammadian, C. Tellambura, and G. Y. Li, "Deep learning-based phase noise compensation in multicarrier systems," *IEEE Wireless Communications Letters*, vol. 10, no. 10, pp. 2110–2114, 2021.
- [18] Mathworks, Inc., "Matlab 5G Toolbox," <https://www.mathworks.com/products/5g.html>, 2020.
- [19] 3GPP TR 38.901, "Study on channel model for frequencies from 0.5 to 100 GHz (Release 16)," v16.0.0, Dec. 2019.